Available online at www.sciencedirect.com
ScienceDirect
Earth and Planetary Science Letters 264 (2007) 46–60
EPSL
www.elsevier.com/locate/epsl

The role of gas percolation in quiescent degassing of persistently active basaltic volcanoes

M.R. Burton [a,*], H.M. Mader [b], M. Polacci [a]

[a] Istituto Nazionale di Geofisica e Vulcanologia, Sezione di Catania, Piazza Roma, 2, Catania, 95123, Italy
[b] Department of Earth Sciences, University of Bristol, Wills Memorial Building, Queens Road, Bristol BS8 1RJ, UK

Received 10 May 2006; received in revised form 16 August 2007; accepted 28 August 2007
Available online 8 September 2007
Editor: C.P. Jaupart

Abstract

Using constraints from literature data on the petrology and texture of erupted material from Stromboli and geochemical measurements of gas emissions together with a model of gas solubility we construct a conceptual model of quiescent degassing for this volcano. We find that within a pressure range between 100 MPa and 50 MPa (~3.6 km and ~1.8 km depth respectively) vesiculating magma ascending within the conduit becomes permeable to gas flow and a transition from closed- to open-system degassing takes place. Above the transition, gas, rich in the most insoluble gases, flows up through degassing magma, and thereby becomes enriched in more soluble gases during ascent to the surface. The final gas emission is therefore a superposition of gases released from magma above the percolation transition and gas that has evolved in closed-system below the transition.

Steady-state gas release from Stromboli can only be sustained via magma circulation, driven by the density variation between ascending vesiculating magma and descending degassed magma. By balancing the buoyant force of ascending vesiculating magma against the viscous resistance produced by travelling through descending, degassed magma in a simple flow model we determine that a cylindrical conduit diameter of 2.5–2.9 m produces the magma mass flow rate of 575 kg s^{-1}, required to account for the observed quiescent SO_2 gas flux on Stromboli of ~2.3 kg s^{-1} (200 td^{-1}).

Keywords: volcanology; magmatic degassing; persistent activity; magma circulation; Stromboli

1. Introduction

Over timescales of years, persistently active basaltic volcanoes such as Etna (Eastern Sicily, Italy) and Stromboli (Aeolian Archipelago, Italy) produce more gas during quiescent activity than during eruptions (Francis et al., 1993). Allard (1997) estimated that ~80% of gas emissions were generated by magma that never erupted on Etna, and the figure is even higher for Stromboli (Allard et al., 1994). Recent technological developments (Francis et al., 1998; Galle et al., 2003) allow regular remote sensing measurements of the composition and flux of magmatic volatiles from quiescently degassing systems. The variations observed in these new data require a deeper understanding of quiescent degassing processes for complete interpretation.

Previous work on magmatic degassing has highlighted the important role of a transition from open- to closed-system degassing in controlling transitions from effusive to explosive activity. Open-system degassing is associated

* Corresponding author. Istituto Nazionale di Geofisica e Vulcanologia, Sezione di Catania, Piazza Roma 2, 95123, Catania, Italy.
E-mail address: burton@ct.ingv.it (M.R. Burton).

0012-821X/$ - see front matter © 2007 Elsevier B.V. All rights reserved.
doi:10.1016/j.epsl.2007.08.028

with effusive behaviour as gas escapes along porous conduit–magma interfaces and through porous magmas (Eichelberger et al., 1986; Jaupart and Allegre, 1991; Woods and Koyaguchi, 1994; Jaupart, 1998; Gonnermann and Manga, 2003; Rust et al., 2004). A debate has taken place on the degassing mechanisms that produce different types of explosive activity in basaltic systems, ranging from Strombolian activity to lava fountains. Parfitt (2004) summarised two models of explosive activity, the rise speed dependent model (Parfitt and Wilson, 1995) and the foam layer collapse model (Jaupart and Vergniolle, 1988, 1989) (which was recently invoked to interpret gas measurements of a lava fountain on Etna Allard et al., 2005). Several studies (Kazahaya et al., 1994; Harris and Stevenson, 1997; Stevenson and Blake, 1998) have also discussed the role of density-driven overturn in persistently degassing basaltic systems, but until now there have been few attempts at quantitative determination of the physico-chemical nature of the magma/gas mixture undergoing such overturn.

The objective of this paper is to combine information on the nature of volatile exsolution from petrological (Métrich et al., 2001; Bertagnini et al., 2003; Landi et al., 2004), textural (Lautze and Houghton, 2005, 2007; Polacci et al., 2006a,b, in press) and geochemical studies (Burton et al., 2007) with fluid mechanical considerations in order to constrain a conceptual steady-state model of quiescent magma degassing in basaltic systems, focussing particularly on Stromboli. Stromboli is the archetype for persistent, passive degassing interspersed with mild, regular explosive activity and more rare major and paroxystic explosions and effusive eruptions (Barberi et al., 1993). In the following we first present constraints placed on the degassing process at Stromboli from a range of recent field observations and analyses of eruption products. We then use these constraints together with a gas solubility model to determine the vesicularity of magma undergoing closed-system degassing. Combining these results with considerations from gas permeability modelling allows us to estimate the pressure range in which a transition from closed- to open-system degassing takes place. The resulting density profile allows us to use a simple conduit flow model to constrain the geometry of Stromboli's conduit. We then use this model to examine the lifetime of magma in the conduit system, investigate the processes producing zoned plagioclase (Landi et al., 2004) and interpret the degassing signature observed in the quiescent SO_2/HCl ratio (Burton et al., 2007). Finally, we investigate timescales of magma ascent and shallow residence, as well as bubble rise speeds and slug coalescence.

2. Constraints

Here we consider the constraints placed on the degassing process at Stromboli from (Section 2.1) petrology, focussing on primitive and final dissolved volatile contents of magma to determine the exsolved volatile content; (Section 2.2) textural studies of scoria, to determine the nature of magma vesiculation in the shallow conduit; (Section 2.3) gas geochemistry, to examine if the observed gas composition is consistent with closed-system degassing, to constrain the original CO_2 content of magma, and to calculate the magma supply rate based on the flux of SO_2.

2.1. Petrological constraints

In order to constrain the degassing process we must know the original and final volatile contents of the magma, which allows us to determine how much gas will be produced during its ascent to the surface. Original dissolved volatile contents can be determined by measuring melt inclusions (MI) trapped at high pressure in primitive olivine crystals that are brought to the surface during major and paroxystic explosions on Stromboli. Métrich et al. (2001) and Bertagnini et al. (2003) report numerous detailed measurements on volatile contents of such MI, successfully constraining primitive concentrations of H_2O, S and Cl. CO_2 is highly insoluble and had already been extensively degassed from even the most primitive samples, making determination of the original dissolved amount impossible through direct measurement. Measurements of the volatile contents of glass in scoria (Métrich et al., 2001; Landi et al., 2004) erupted during mild Strombolian activity constrain the final volatile contents of magma in the shallow conduit. The results from these studies and derived calculations are reported in Table 1.

K_2O contents of scoria glass (4–5 wt.%) are consistent with the expected increase of this incompatible element due to crystallization of ~50% of the original melt. Landi et al. (2004) report a phenocryst content of 47–55 vol.% in scoria from Stromboli, with plagioclase being most abundant (57–71 vol.%), followed by clinopyroxene (20–34 vol.%) and olivine (4–12 vol.%).

Zonation of plagioclase crystals into layers of skeletal light grey bytownitic and dark grey labradoritic material was shown (Landi et al., 2004) to be evidence of a complex magma supply consistent with cyclic crystal growth in two different magmas, with $H_2O < 1.6$ wt.% and $H_2O < 0.6$ wt.%, respectively. Skeletal features of bytownitic cores and concentric zones are consistent with rapid gas loss.

Table 1
Summary of measured volatile contents and degassing volumes

	[a]Original volatile content (melt inclusions)			[b]Final volatile content (scoria, whole rock)	Max exsolved volatiles			[c]Max exsolved gas volume per volume of magma
	C_o			C_f	$\Delta C = C_o - C_f$	$100 \times \Delta C/C_o$		
	(wt.%)	(kg m^{-3})	(mol m^{-3})	(wt.%)	(wt.%)	(% of Co)	(mol m^{-3})	
H_2O	3.67	91.75	5097.22	0.05 (Allard et al., 2005)	3.62	98.63%	5027.78	573.16
CO_2	2.44 (Allard et al., 1994; Bertagnini et al., 2003)	61.00	1386.36	0.005 (Allard et al., 2005)	2.435	99.80%	1383.52	157.57
S	0.16–0.23 (Allard et al., 2005; Kazahaya et al., 1994)	5.75	179.69	0.003–0.03 (Harris and Stevenson, 1997)	0.20	98.70%	156.25	17.80
Cl	0.17–0.20 (Allard et al., 2005; Kazahaya et al., 1994)	5.00	140.85	0.036–0.065 (Harris and Stevenson, 1997)	0.164	82.00%	115.49	13.15
K_2O	1.6–2.1 (Kazahaya et al., 1994)	156.75	6429.12	1.92–2.07 (Harris and Stevenson, 1997)		Total	6683	762

[a] Concentrations were measured in melt inclusions within primitive olivine crystals and corrected for post-entrapment crystallisation by (Métrich et al., 2001; Bertagnini et al., 2003), apart from CO_2 which is derived from gas measurements by (Allard et al., 1994; Burton et al., 2007) and in Section 2.3, and H_2O which is derived by a measured concentration of 3.2 wt.% from (Bertagnini et al., 2003) and adding a calculated pre-existing exsolved H_2O gas content calculated from VolatileCalc and the primitive CO_2 content (Section 3). Original volatile content in wt.% was determined assuming a magma density of 2500 kg m^{-3}.

[b] Concentrations in scoria are derived from (Landi et al., 2004) using S and Cl concentrations in glasses and correcting to whole rock concentrations.

[c] The maximum volume of exsolved gas was calculated using the ideal gas law at a temperature of 1115 °C and atmospheric pressure.

Métrich et al. (2001) estimated several physical parameters for Strombolian magmas that we use in our calculations. The original uncrystallised magma was estimated to have a viscosity of 20–30 Pa s, a density of 2500 kg m^{-3} and a temperature of 1145 °C. The shallow, degassed, 50% crystallised magma was estimated to have a viscosity of ~14,000 Pa s, a density of 2700 kg m^{-3} and a temperature of 1115 °C. A viscosity of ~14,000 Pa s for degassed magma agrees well with laboratory and theoretical calculations of the viscosity of basaltic melts and crystal-bearing magmas. For Stromboli degassed magma at T=1115 °C and H_2O=0.1–0.2 wt.%, the equation of (Giordano and Dingwell, 2003) provides a melt viscosity of ~200 Pa s. (Costa et al., 2007) showed that the viscosity of magmas with crystal content ~50% is found to be two orders of magnitude higher than that of the related liquid, implying a viscosity of ~20,000 Pa s for Stromboli's degassed magma. On the contrary, much lower viscosity estimates of 300 Pa s for the magma layer around each explosive gas slug have been obtained via acoustic measurements (Vergniolle et al., 1996). We show below that the explosion products contain an appreciable amount of bubbles as well as crystals. The rheology of three-phase suspensions such as this has not been measured. However the rheological effect of adding either crystals or bubbles separately (i.e. two-phase suspensions) has been observed. Both are found to be strongly shear-thinning. The viscosity at high strain rates of a ~50 vol.% suspension of either crystals or bubbles is less than at low strain rates by ~ one order of magnitude (Caricchi et al., in press; Llewellin et al., 2002a,b, 2003; Rust and Manga, 2002). Moreover bubble suspensions are viscoelastic and imposed oscillations, such as the seismic vibrations commonly associated with slug rise (Vergniolle et al., 1996), will also cause a reduction in the viscosity by as much as ~one order of magnitude (Llewellin et al., 2002a,b, 2003). It is not known how these effects combine in concentrated three-phase suspensions. Nevertheless, the lower viscosity estimates in (Vergniolle et al., 1996) are probably indicative of high strain rate conditions around exploding slugs in the shallow bubble-rich magma. By contrast, quiescent degassing processes occur at low strain rate. Therefore, 14,000 Pa s remains the most appropriate estimate for the viscosity of the sinking degassed magma, and this value is used throughout this work.

2.2. Textural constraints

Recent studies (Lautze and Houghton, 2005, 2007; Polacci et al., 2006a) of the textures of products from mild explosive activity on Stromboli and Etna have shed

new light on the dynamics of their shallow feeding systems and give fundamental constraints to degassing models. These products do not show any evidence of post-eruptive degassing processes, i.e. expansion features indicated by bread-crusted surfaces or vesicularity gradients from clast centre to rim, therefore we assume that they are representative of the actual state of magma in the uppermost part of the conduit.

Lautze and Houghton (2005, 2007) found that tephras from Strombolian explosions in 2002 at Stromboli are characterized by two end-members, low- (LD) and high- (HD) density scoriae, as well as by products that represent a mingling of the two textures. LD scoriae are described to possess a bimodal bubble size distribution with a population of smaller, spherical to sub-spherical bubbles with diameter 0.03–1 mm, and larger bubbles with complex, irregular shapes ranging 2.5–10 mm in diameter. HD scoriae have unimodal bubble size distributions with the larger bubble population described for the LD scoria type making up most of the bubble volume fraction.

3D scoria volumes of the 2005 Stromboli explosive activity reconstructed via X-ray tomographic imaging (see Polacci et al., 2006b for the methodology) show that these ejecta are also HD to LD (~0.40–0.70 bubble volume fraction) clasts with bubble number densities between 10^{10} m^{-3} and 10^{11} m^{-3} and crystal content >40 vol.% (Polacci et al., in press). However, visualization of their 3D microstructure has revealed that >0.90 of the bubble volume fraction is interconnected, consisting of a network of small to intermediate coalescing bubbles that form mostly irregularly-shaped, convoluted, larger individuals. The bulk of the remaining bubbles are spherical, have a diameter <0.1 mm and make up the majority of the number density. The nature of these smaller bubbles is consistent with a late-stage shallow nucleation, given their spherical non-coalesced morphology and small size.

The results from tomographic measurements (Polacci et al., 2006b, in press) are in reasonable agreement with the observations of (Lautze and Houghton, 2005, 2007), but the ability to visualise in 3D highlights the interconnected nature of the majority of the bubble volume fraction (see Fig. 5 in Section 4.3 as an example) in both LD and HD scoria.

The bubble number density of CO_2-rich bubbles in magma at high pressures is difficult to constrain, but important for calculating bubble rise speeds in depressurising magmas. Recent experimental laboratory studies of vesiculation in samples of pumice from a major explosion on Stromboli (Polacci et al., in press) indicate that typical number densities of ~10^{11} m^{-3} are observed for bubbles in water-saturated melts during decompression from 1000 to 370 MPa. We use this observation to estimate the order of the bubble number density produced by high pressure CO_2 nucleation.

In summary, textural observations allow us to state that (i) small, spherical bubbles in scoria are the result of late-stage bubble nucleation; (ii) networks of interconnected bubbles are present in both LD and HD scoria products; (iii) the assemblage is highly permeable to gas flow; (iv) ~10^{11} m^{-3} is a reasonable estimation for the initial bubble number density produced by high pressure CO_2 nucleation.

2.3. Geochemical constraints

The flux and composition of gas emitted during passive degassing gives further fundamental constraints on the feeding system of Stromboli. Degassing takes place via three modes: quiescent degassing directly from magma via the open-conduits, explosive degassing produced by gas slugs rising from 1–3 km depth (Burton et al., 2007) and quiescent degassing from the shallow hydrothermal system (Allard et al., 1994).

Allard et al. (1994) showed that >95% of the total flux of SO_2 came from quiescent degassing of magma through the open-conduit system of Stromboli. Low temperature water-saturated fumaroles around the summit craters of Stromboli are not significant sources of SO_2, but may contribute meteoric water to the total plume (Burton et al., 2007). During 2006 the average flux was ~200 t/d (Burton et al., in preparation) or ~2.3 kg s^{-1} which we assume to be typical of steady-state degassing of Stromboli as there was no anomalous eruptive activity during 2006. Using the amount of S lost during decompression (0.2 wt.%, Table 1) we may deduce the supply rate of primitive magma required to produce such gas fluxes. One m^3 of primitive magma with a density of 2500 kg m^{-3} will exsolve $0.2 \times 0.01 \times 2500$ kg = 5.0 kg of S, which will oxidize to produce 10.0 kg of SO_2, since the molecular weight of SO_2 (64 g) is double the atomic weight of S (32 g). An SO_2 flux of 2.3 kg s^{-1} therefore requires complete degassing of (2.3 kg s^{-1}/10.0 kg m^{-3}) × 2500 kg m^{-3} = 575 kg s^{-1} of primitive magma.

We may estimate the total CO_2 amount by assuming that input magma degasses all its CO_2 and SO_2 during ascent to the surface (bulk degassing), producing a gas composition that is indicative of the original CO_2 content. A CO_2/SO_2 molar ratio of 7.8 was measured on Stromboli using passive open-path FTIR measurements (Burton et al., 2007) during quiescent degassing, equivalent to a CO_2/S weight ratio of 10.7. Using the amount

of exsolved S of 0.20 wt.% reported in Table 1 allows us to estimate the original CO_2 content to be 2.44 wt.%, assuming bulk degassing. This is much higher than the maximum value of 0.16 wt.% dissolved in the most primitive melt inclusions (Métrich et al., 2001; Bertagnini et al., 2003), but is compatible with recent work which postulates that original CO_2 concentrations may be much greater than those measured in primitive melt inclusions (Papale, 2005), that are in any case minimum values of the total gas content (Wallace, 2005).

Measurements of gas emissions from the central vents of Stromboli with FTIR show that the SO_2/HCl ratio for quiescent degassing is 1.7–1.8 (Burton et al., 2007). The petrological values reported in Table 1 show that a complete bulk degassing would produce a gas with a S/Cl weight ratio of 1.38 and therefore a SO_2/HCl molar ratio of 1.54, similar to the observed value of 1.7–1.8 given by (Burton et al., 2007). Therefore, to a good approximation SO_2/HCl observations evidence a bulk degassing composition.

3. Closed-versus open-system degassing

In the following we calculate the amount of volatiles exsolved during magma ascent in a closed-system per unit volume of magma, and compare with constraints from textural studies. The VolatileCalc model (Newman and Lowenstern, 2002) calculates the solubility of H_2O and CO_2 as a function of pressure. An SiO_2 content of 49 wt.% and a constant temperature of 1115 °C was used throughout. We initialised a VolatileCalc closed-system degassing path calculation using dissolved amounts of 3.2 wt.% H_2O and 1300 ppm CO_2 (Métrich et al., 2001; Bertagnini et al., 2003), for which the model determined a pressure of 360 MPa and a CO_2/H_2O weight ratio in the equilibrium gas phase of 4.9. The primitive CO_2 content was calculated above in Section 2.3 to be 2.44 wt.%, implying that at 360 MPa 2.31 wt.% CO_2 is already in the gas phase, together with 2.31 wt.%/4.9=0.47 wt.% H_2O. This calculation therefore suggests that the actual primitive amount of H_2O dissolved in Stromboli melt is (3.20+0.47)wt.%=3.67 wt.%.

From this starting point the detailed degassing path for depressurizing magma is calculated between 200 MPa and the surface for 100 levels with 2 MPa spacing. This pressure range was chosen as it covers the largest variations in H_2O solubility and, as we will show, magma vesicularity. The results from the model are shown in Fig. 1a as the variation in dissolved wt.% of CO_2 and H_2O with respect to pressure. Exsolved wt.% of these gases is calculated as the difference between original and dissolved amounts. Almost all CO_2 is already in the gas phase at 200 MPa, and >50% of H_2O is degassed at ~40 MPa. Using these solubility curves we may determine for a unit volume of magma with density 2500 kg m^{-3} how much of each volatile is in the gas phase at any specific pressure. To determine the volume occupied by the gas we use the equation of state for CO_2 and H_2O derived by (Pitzer and Sterner, 1994). The volume occupied by 1 mol of gas (molar volume, V_m) as a function of pressure is shown for CO_2 and H_2O in Fig. 1b. Note that while H_2O shows quasi-ideal behaviour, CO_2 is more incompressible, occupying almost 11% more V_m compared with H_2O at 50 MPa.

Vesicularity is defined as the gas volume divided by the total volume of gas and magma and is shown in Fig. 1c. A vesicularity of 0.50 is reached at a pressure of 50 MPa, and 0.30 vesicularity at ~100 MPa. At 1 bar we calculate that 1 m^3 of magma will produce 762 m^3 of total gas (see Table 1). If all this gas remained in closed-system with the parent magma we would expect to see a scoria vesicularity of 762 m^3/763 m^3 ~0.999. The products of mild Strombolian activity are clearly far denser, possessing vesicularities of 0.40–0.70 (see Section 2.2) We conclude that purely closed-system degassing cannot explain the nature of gas release during magma ascent in the shallow conduit of Stromboli. At some point within the magma feeding system gas must be separating from magma and ascending faster. This appears to be incompatible with the observed SO_2/HCl ratio on Stromboli, as open-system degassing from magma at high pressure would favour higher SO_2/HCl ratios. Resolving this contradiction is one of the objectives of the discussion below.

4. Discussion

In the following we attempt to constrain the physical characteristics of magma ascent, degassing and descent within a cylindrical conduit, based on the Stromboli system. The actual Stromboli plumbing system may differ from the simple cylindrical geometry assumed here. However we imagine that during the long history of persistent activity on Stromboli any inefficiencies in the feeding system would tend to be removed, producing the most energetically favourable method of degassing magma, which may well be a cylindrical conduit. Mass is conserved and we assume the system is in a steady-state condition (Allard et al., 1994; Harris and Stevenson, 1997). We also assume that no gas is lost through the walls of the conduit and that the level of magma within the conduit remains constant. Our model is calculated over a pressure range from 200 MPa to the surface,

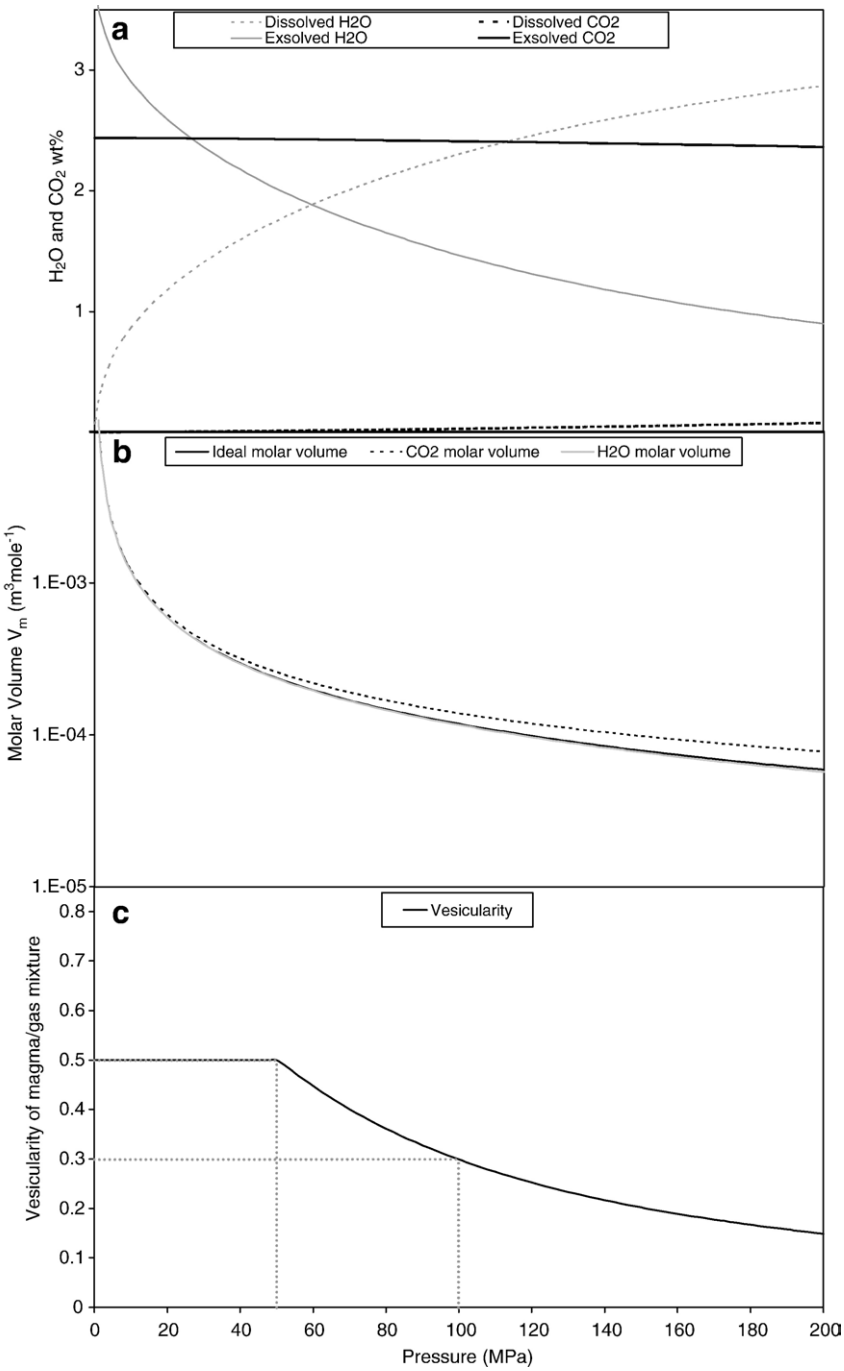

Fig. 1. Calculated pressure-dependent behaviour during closed-system magma decompression: (a) Exsolved and dissolved wt.% of CO_2 and H_2O calculated by VolatileCalc (Newman and Lowenstern, 2002); (b) Non-ideal behaviour of CO_2 and H_2O at 1145 °C calculated using the temperature-dependent second virial coefficient calculated from (Pitzer and Sterner, 1994); (c) Vesicularity calculated as gas volume divided by total gas and magma volume, with pressures associated with vesicularities of 0.30 and 0.50 highlighted with dashed lines.

chosen as this is the range in which we find vesicularity variations play a dominant role. From a consideration of permeability development (Section 4.2) we fix the transition from closed- to open-system degassing to a vesicularity of 0.50, below which exsolving gas remains in closed-system, and above which gas escapes through percolation such that thereafter the vesicularity of 0.50 is maintained in the ascending magma.

We first investigate the bubble rise rate prior to the open-system degassing transition and discuss how this is related to the initial bubble number density. We then use our calculations of vesicularity to constrain the density-driven magma overturn rate below the transition point, and use mass conservation to determine the conduit radius as a function of pressure. We discuss the relationship between vesicularity and permeability, the transition from closed- to open-system degassing and the possibility that bubble networks may collapse to form gas-bearing channels. Finally, we examine volatile exsolution at low pressure and compare with textural observations in scoria.

4.1. Pre-transition bubble rise rate and magma circulation

Gas bubbles may rise relative to their source magma during magma ascent. Bubbles of various sizes rise at different rates and may coalesce to form gas slugs. Parfitt (2004) used this rise speed dependent model to explain Strombolian activity as the consequence of such gas slugs fragmenting near the surface. We may use our degassing model to examine the typical bubble radius during decompression, if we assume that degassing occurs exclusively into pre-existing bubbles and if we specify the original bubble number density. With the calculated bubble radii, and given an estimate for magma viscosity and the density difference between the gas bubble and surrounding magma, we may deduce the bubble rise speed and hence assess the potential relevance of the rise speed dependent model for slug genesis at Stromboli.

The low solubility of CO_2 in basalt suggests that nucleation of pure CO_2 bubbles will take place under great pressures; to dissolve 2 wt.% of CO_2 in a basalt requires a pressure greater than 20 kbar or ~2000 MPa (Blank and Brooker, 1994) equivalent to ~60 km depth. CO_2 must therefore exsolve at great depth, prior to degassing of other volatile components, producing magma with a certain initial bubble number density (bnd), n_o, defined as the number of bubbles per total volume of gas and magma. We assume that as magma slowly ascends in closed-system, it is energetically favourable to exsolve other gas species into these pre-existing bubbles, rather than nucleate new bubbles (Mourtada-Bonnefoi and Mader, 2004), and that the total number of bubbles formed at depth remains constant until coalescence and the transition to open-system degassing. It is worth noting that, as the bubbles rise and grow, the bnd reduces, because the total volume increases but no new bubbles are formed. In general, the bnd n is given by $n=(1-\phi)n_o$, where ϕ is the vesicularity.

Let us examine the fundamental role that the bubble number density plays in determining the bubble rise rate. First we calculate the bubble radius r_b by assuming that all bubbles in a unit volume have the same size, determined by dividing the vesicularity ϕ, which is the volume of gas per total volume, by the bubble number density n. Hence,

$$\frac{4}{3}\pi r_b^3 = \frac{\phi}{n} = \frac{\phi}{(1-\phi)n_o} \quad (1)$$

The rise velocity of the bubbles is dependent on magma viscosity η, bubble radius and density contrast between the bubble and the magma $\Delta\rho$, as described by Stoke's law:

$$v_b = \frac{2}{9}\frac{g r_b^2 \Delta\rho}{\eta} \quad (2)$$

where g is the acceleration due to gravity. We use $\Delta\rho=2500$ kg m^{-3} and $\eta=20$ Pa s (Section 2.1 Métrich et al., 2001) and $n_o=10^{10}$ and 10^{11} m^{-3} (see Section 2.2). Combining Eqs. (1) and (2) shows that, for given $\Delta\rho$, η and ϕ, the bubble rise velocity $v_b \propto {n_o}^{-2/3}$ and hence a 10-fold increase in n_o produces a change in v_b by a factor of $10^{-2/3}=0.215$, i.e. almost 5-times slower. The calculated velocities for $n_o=10^{10}$ and 10^{11} m^{-3} (see Fig. 2) increase with decreasing pressure due to their increasing radius. Typical bubble rise speeds are $\sim 1.5\times10^{-5}$ ms^{-1} for $n=10^{10}$ and $\sim 3\times10^{-6}$ ms^{-1} for $n=10^{11}$.

The importance of the bubble rise velocity is dependent on the magma ascent rate; if the bubble rise velocity is small relative to the magma ascent rate then bubbles remain with their parent magma during rise and interconnection between bubbles will be hampered. In order to constrain the magma ascent rate we consider the rise of vesicular material up a conduit, which we assume is a simple cylinder of radius R. Koyaguchi and Blake (1989) and Stevenson and Blake (1998) present analogue experiments that involve similar systems. In (Koyaguchi and Blake, 1989) a liquid was forced up a vertical pipe that was filled with another liquid. By contrast, (Stevenson and Blake, 1998) observed buoyant rise of one liquid through a more dense overlying liquid. In the latter experiments, liquid intruding from below was found to flow up the centre of a pipe filled with liquid of a different viscosity when the viscosity ratio between the two liquids was sufficiently large (>~300). This is analogous to the Stromboli system where the viscosity ratio between ascending, degassing, low viscosity magma and descending degassed magma is ~14000 Pa s/20 Pa s=~700. This geometry of flow is

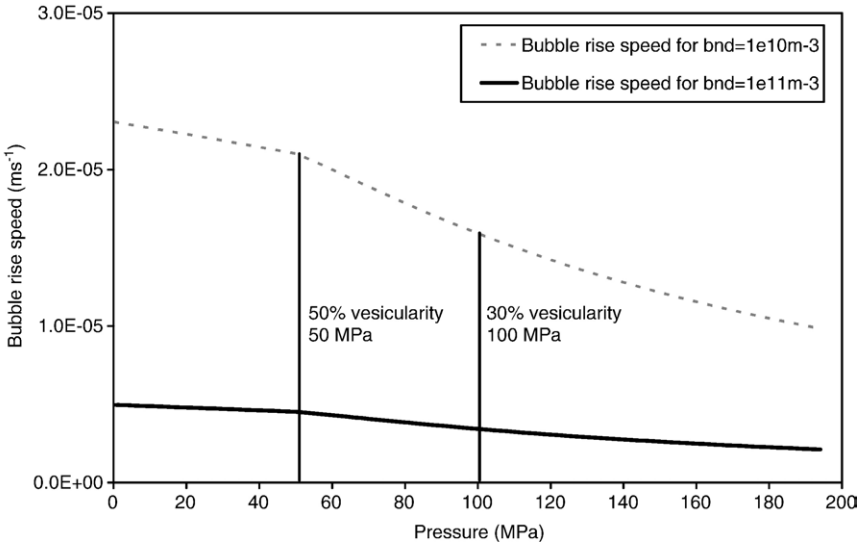

Fig. 2. Bubble radius and rise rate as a function of pressure for two bubble number densities. Note that if bubbles are identical size at a certain pressure then vesicularity is independent of bubble number density.

therefore adopted in the model presented in Fig. 3. Material with vesicularity ϕ flows at a speed v_s up the centre of the conduit occupying a cylindrical region of radius r_s. We hypothesise that the ascending magma produces unerupted, degassed magma that sinks back down the same conduit in the annular region between the rising material and the conduit walls at speed v_d. A key distinction between our model and those of (Koyaguchi and Blake, 1989) and (Stevenson and Blake, 1998) is that we explicitly calculate the density contrast as a pressure-dependent parameter controlled by the developing vesicularity of the ascending magma flow. In (Koyaguchi and Blake, 1989) and (Stevenson and Blake, 1998) the effects of vesiculation are neglected and the driving density contrast is a constant determined from the initial and final dissolved volatile contents, initial bubble density in the magma chamber and final crystal content. We now derive an equation to calculate the magma ascent velocity in our model.

Simple mass balance dictates that the mass of ascending magma is balanced by an equal mass of descending magma (neglecting mass lost through outgassing):

$$v_s r_s^2(1-\phi) = v_d\left(R^2 - r_s^2\right) \tag{3}$$

The rise of the vesicular material is controlled by the balance of viscous and buoyancy forces, F_v and F_b respectively.

The buoyancy force per unit height is, to an order of magnitude:

$$F_b \sim r_s^2 \Delta\rho g \tag{4}$$

where $\Delta\rho = \rho\phi$ is the difference in density between the ascending vesicular magma and the descending degassed magma.

The viscosity of the sinking, degassed magma is likely to be much larger than the viscosity of the vesiculated, partially-degassed magma. This is because degassing and crystallisation cause an increase in viscosity by three orders of magnitude in this case, taking the viscosity of the magma from ~20 Pa s to ~14,000 Pa s (Section 2.1 Métrich et al., 2001), whereas the viscosity increase due to vesiculation is only around one order of magnitude (Llewellin et al., 2002a,b, 2003; Rust and Manga, 2002). Therefore, the dominant viscosity control

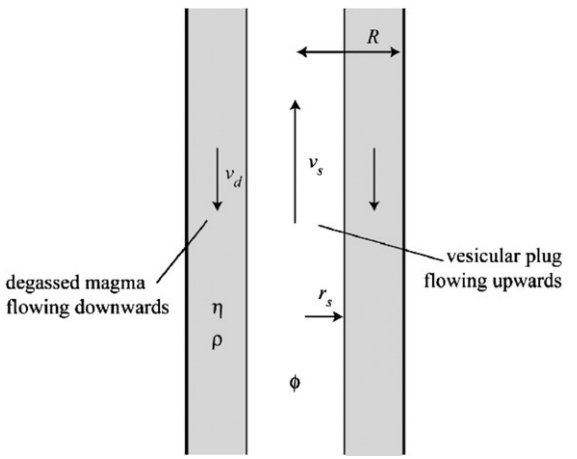

Fig. 3. Vesicular magma rising at a speed v_s up the centre of a conduit with degassed material descending in the surrounding annular region at speed v_d.

is provided by the viscous force in the sinking, degassed fluid.

The viscous force per unit length in the sinking degassed magma is the viscous stress at the vesicular plug wall multiplied by the surface area per unit height of the plug (i.e. its circumference $\sim r_s$). The viscous stress is given by the velocity gradient across $(R-r_s)$ multiplied by the viscosity of the degassed magma η. Hence, we obtain, to an order of magnitude:

$$F_v \sim \frac{v_s + v_d}{R - r_s}\eta r_s \tag{5}$$

Balancing buoyancy (4) and viscosity (5) gives

$$v_s + v_d \sim \frac{\Delta\rho g}{\eta}\left(Rr_s - r_s^2\right) \tag{6}$$

We can estimate the radius of the ascending magma flow by assuming that the flow will adopt a radius such as to maximise its rise velocity relative to the sinking, degassed magma. This occurs when $d(v_s+v_d)/dr_s=0$, i.e. when $r_s=R/2$ in which case

$$v_s + v_d = \frac{\Delta\rho g}{4\eta}R^2 \tag{7}$$

Finding solutions to Eq. (7) for Stromboli requires us first to take account of mass loss through outgassing. We showed in Section 2.3 that the primitive magma input rate on Stromboli is 575 kg s^{-1}. A total of 6.4 wt.% of gas (made up of 3.62 wt.% H_2O, 2.44 wt.% CO_2, 0.20 wt.% S and 0.164 wt.% HCl, see Table 1) is lost during magma ascent, producing an effective $(1-0.064)\times 575 = 538.2$ kg s^{-1} output of degassed magma. Neglecting scoria emission this is the mass flow rate of degassed magma travelling back down the conduit.

The velocity of the ascending magma is a function of the density contrast between ascending and descending magma $\Delta\rho=\rho\phi$ and the conduit radius R. The density contrast for each pressure level is determined from the vesicularity versus pressure relationship shown in Fig. 1c. At each pressure (7) allows us to calculate by inspection the unique conduit radius R that allows vesiculated, ascending magma to achieve a mass flow rate of 575 kg s^{-1} and degassed descending magma to achieve a mass flow rate of 538 kg s^{-1}. We find that the conduit radius is 1.45 m at 200 MPa and decreases to 1.28 m at 50 MPa, (Fig. 4). The radius remains constant at lower pressures due to the steady density contrast imposed by the fixed vesicularity of 0.50 associated with gas percolation (see Section 4.0). A radius of 1.3–1.5 m is comparable to that reported from observations of explosions (Chouet et al., 1974) and acoustic measurements (Vergniolle and Brandeis, 1996).

The magma ascent velocity (see Fig. 4) increases with decreasing pressure as the density contrast between vesiculating and degassed magmas develops. Ascent velocities increase from 0.18 ms^{-1} at 200 MPa to 0.37 ms^{-1} at 50 MPa. Descent velocities of degassed magma are slower, due to higher density, lack of bubbles and greater area occupied in the annulus of the conduit. At 50 MPa the descent velocity is 0.053 ms^{-1} and at 200 MPa 0.041 ms^{-1}. We note that the Reynolds

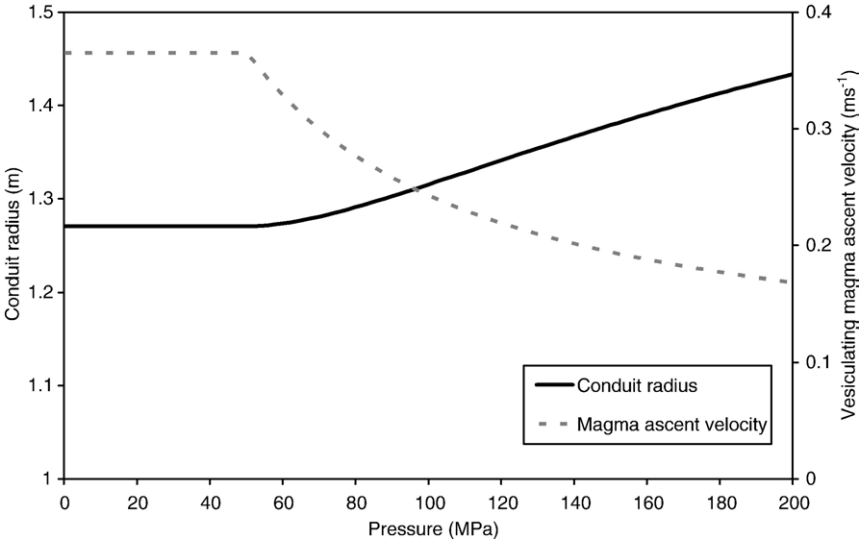

Fig. 4. Vesiculating magma ascent rate and conduit radius as a function of pressure.

numbers in all regions are <100, so the inherent assumption in our analysis of laminar flow conditions is justified.

These magma ascent velocities are ~5 orders of magnitude greater than calculated bubble rise speeds of $\sim 1.5\times10^{-5}$ ms^{-1} for $n=10^{10}$ and $\sim 3\times10^{-6}$ ms^{-1} for $n=10^{11}$. Timescales for magma ascent may be estimated by using the average velocity of ascending magma between 200 MPa and 50 MPa; from inspection of Fig. 4 this is ~0.22 ms^{-1}. Assuming a lithospheric density of 2750 kg m^{-3} these pressures are equivalent to depths of 7.3 km and 1.8 km. The ascent to the gas percolation transition would therefore take (7300–1800)m/0.22 ms^{-1}=25,000 s or ~7 h. Further ascent to the surface takes place over ~1.4 h. The short timescale for ascent from 200 MPa to 50 MPa may partially explain the scarcity of trapped melt inclusions from this pressure range in natural samples (Métrich et al., 2001; Bertagnini et al., 2003). Bubbles would therefore cover a distance of ~0.35 m and ~0.07 m for bubble number densities of 10^{10} m^{-3} and 10^{11} m^{-3} respectively during magma ascent from 200 MPa to 50 MPa. This assumes all bubbles are the same size at any given pressure step. In reality a range of sizes will coexist, with a range of speeds enhancing the probability of coalescence events (Parfitt, 2004). However, given the limited timescale, it seems likely that the greatest number of collisions will occur at lowest pressures, where the rise speed is greatest. Therefore, both the size distribution and number density of the deep initial bubble nucleation play a critical role in determining magma/gas dynamics at shallower levels.

If the gas slug genesis process that produces Strombolian activity was controlled primarily by rise speed dependent collision events (Parfitt, 2004) we may reasonably expect that slugs would mostly form immediately below the percolation threshold. Measurements of the gas phase released by slugs during explosive activity on Stromboli (Burton et al., 2007) show that the source pressure for gas slugs driving the most explosive activity lies within the pressure range proposed here for the transition to open-system degassing, 70–80 MPa. Such pressures are consistent with the volcano–crust interface depth (Burton et al., 2007), suggesting that a structural control may play a role in slug coalescence via foam accumulation (Jaupart and Vergniolle, 1988, 1989). The transition to percolation gas flow may itself promote slug coalescence if pockets of interconnected bubbles coalesce through bubble expansion prior to full connection with the main degassing pathways. We conclude that in the transition region several mechanisms may combine to encourage slug coalescence.

4.2. Vesicularity and permeability

Many studies have examined the relationship between permeability and vesicularity, both theoretically (Sur et al., 1976; Rintoul and Torquato, 1997; Blower, 2001; Costa, 2006; Gaonac'h et al., 2003) and on natural samples (Klug and Cashman, 1996; Saar and Manga, 1999; Mueller et al., 2005), finding that there is a highly non-linear relationship between the two properties.

We assume that for slowly ascending magmas, bubbles will be spherical. Blower (2001) presents a model that calculates the porosity for randomly-sited bubbles, and finds that the percolation threshold is at a vesicularity of 0.30 and independent of the bubble size distribution in agreement with other researchers (Sur et al., 1976; Rintoul and Torquato, 1997). However, maximum permeability for a network of spherical bubbles requires significantly higher gas volume fractions. The above studies show that, when ~0.50 vesicularity is achieved, the system, regardless of the size, shape or distribution of the bubbles, will be highly permeable and allows efficient gas percolation. Using Fig. 1c, we see that 0.30 vesicularity is achieved at a pressure of 100 MPa, and 0.50 vesicularity at 50 MPa. We therefore conclude that the transition from closed- to open-system degassing occurs over the depth range associated with the change in pressure from 50 to 100 MPa.

4.3. Closed- to open-system degassing transition and gas flow rate

The rapid ascent of magma calculated in our flow model implies a rapid exsolution of water; when the water concentration drops to <1.6 wt.% at a pressure of ~40 MPa, plagioclase will begin to crystallise, producing bytownitic, skeletal crystals, as seen in the cores of zoned plagioclase on Stromboli (Landi et al., 2004). Rapid crystallization and continuing water loss will induce a rapid increase in melt viscosity, by up to 3 orders of magnitude. In the percolation region, ascending and degassing melt will become a decreasingly important source of gas compared with the gas flowing through the magma from below. This may induce an evolution from a highly vesiculated magma to a magma filled with percolation channels (Polacci et al., in press), that may open and close dynamically in order to release the gas pressure from below. Such structures are directly observed in eruption products (Polacci et al., in press). In Fig. 5 we see an example of one of these channel-like features, revealed with X-ray tomography (see Section 2.2). The dynamic nature of the channel structures would allow rapid reformation after being disrupted by the passage of a gas slug.

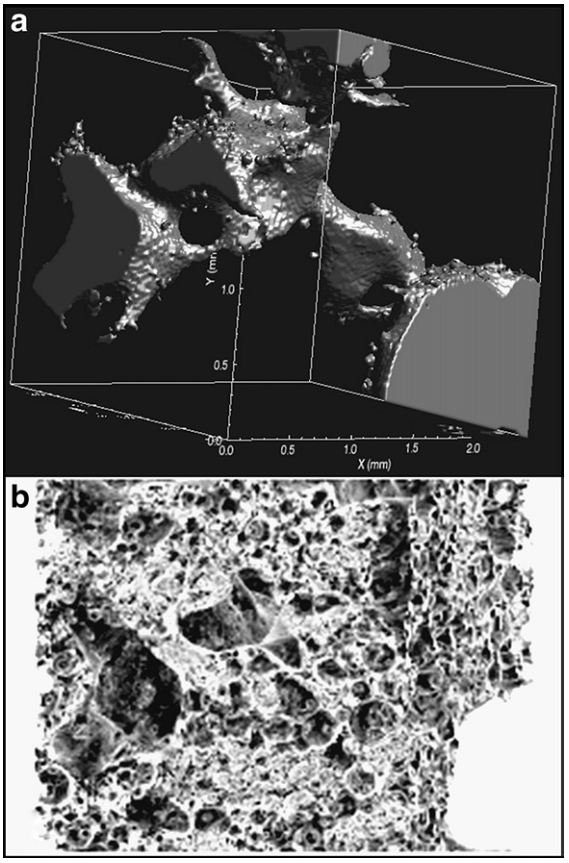

Fig. 5. 3D reconstructed volume of a scoria sample from Stromboli via X-ray tomographic imaging: (a) interconnected bubbles within the scoria sample; (b) volume rendering of the sample from the same angle and scale. Note that superficial voids in (b) are internally connected, producing an open channel through the sample.

We may estimate the gas flow rate within our model. Below the gas percolation transition, gas will ascend essentially together with magma, because the bubble rise velocity ($\sim 1\times10^{-5}$ ms^{-1}) is much less than the magma ascent velocity (~ 0.3 ms^{-1}). A minimum gas velocity above the transition may be calculated by determining the exsolved gas volume flux at each pressure. This is done by multiplying the magma input rate (575 kg s^{-1}) with the volume of exsolved gas produced per kg of primitive magma as a function of pressure. The effective flow area open to percolation can be estimated as the cross-sectional area of the ascending magma multiplied with porosity. Dividing the gas flux at each pressure level with the effective flow area gives the gas velocity shown in Fig. 6. We see that the gas velocity strongly increases at shallow depths. Gas flow, together with the dynamics of opening and closing channels in the permeable ascending magma, are both potential seismogenetic sources and could potentially produce volcanic tremor. The calculated peak velocity at the surface of ~ 280 ms^{-1} is likely to be an overestimate as the conduit is much wider near the surface, providing a larger free surface for degassing, as described in detail in the following section.

4.4. Shallow degassing processes

Melt inclusion studies of Etnean magmas show that the majority of dissolved HCl and HF exsolve at pressures <15 MPa (Metrich et al., 2004). Gardner et al. (2006) showed that while Cl is highly soluble at low pressure, the presence of a permeable gas flow promotes efficient Cl exsolution. Assuming the solubilities of HCl and HF are broadly similar in Strombolian magmas we expect that halogens are primarily sourced in the shallowest part of the conduit system. The SO_2/HCl ratios on Stromboli are controlled therefore by the superposition of a deep-sourced SO_2-rich gas flux and a shallow-sourced HCl-rich gas flux. In steady-state conditions with constant magma supply rising from depth to the surface these fluxes produce the bulk degassing signature SO_2/HCl ratio of 1.5–2. This implies that the average ascending magma flux close to the top of the conduit is similar to that at depth, and that ascending magma arrives at the top of the magma column before sinking back down. The SO_2/HCl ratio measured during quiescent degassing is therefore an important constraint on the magma dynamics within Stromboli. An increase in magma supply rate may be seen at the surface as an increase in SO_2 flux, before any change in activity, as this gas ascends quicker than the ascending magma. This will therefore induce an increase in measured SO_2/HCl ratio during quiescent degassing. On the contrary, if the magma supply rate slows then we may see a decrease in SO_2/HCl ratio. Such processes may therefore be important for interpreting variations in SO_2/HCl during quiescent degassing for basaltic systems in general.

The large crater terrace, multiple gas emission points, location of very long period seismic signals (Chouet et al., 2003) and voluminous lava effusion observed during the 2002/03 (Landi et al., 2006) and 2007 eruptions evidence probable widening of the superficial conduit system on Stromboli, suggesting that the potential volume of the shallowest (<250 m) conduit is larger than that used in our simple model. Observations made of the volume of lava outpouring in the first days during both the 2002/03 (Landi et al., 2006) and 2007 eruptions of Stromboli suggest that the total volume of magma resident in the shallow region is $\sim 2\times10^{6}$ m^{3}. This implies that, for a magma input rate of ~ 575 kg s^{-1} and a vesicularity of ~ 0.50 for both resident magma and

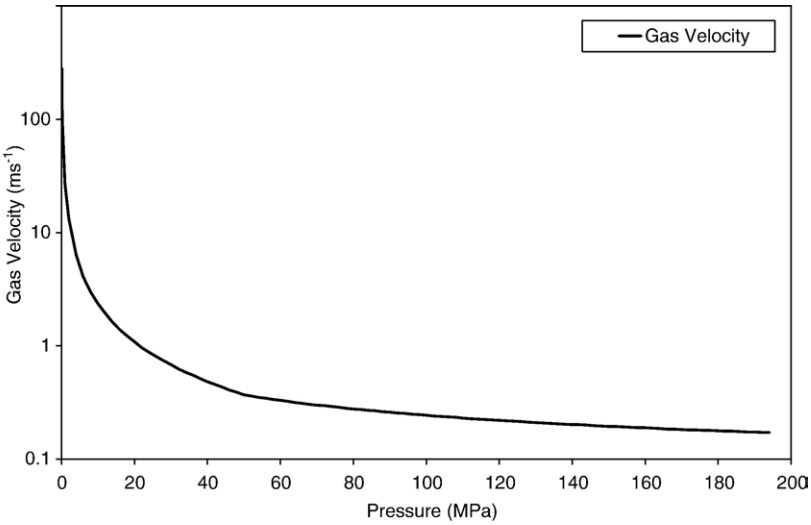

Fig. 6. Calculated gas velocity within the conduit.

initial outpouring lava, the average lifetime of magma in the uppermost 250 m of the conduit system is ~50 days. Francalanci et al. (1999) calculated a longer magma lifetime of 19 years based on smooth variations in $^{87}Sr/^{86}Sr$ ratios of erupted scoria and lavas, which clearly points to a well-mixed magma reservoir that buffers the Sr ratio. Therefore, while the shallowest magma may be rapidly flushed, the roots of the conduit system are probably fed by a buffering magma reservoir. Armienti et al. (2007) used the 19-year timescale determined by (Francalanci et al., 1999) to calculate plagioclase growth rates based on crystal size distributions on Stromboli, and found values 1–2 orders of magnitude lower than literature values. Instead, using a lifetime of ~50 days produces growth rates consistent with the literature, supporting our hypothesis of rapidly flushed shallow plagioclase-forming magma.

4.5. Magma recycling

Below the percolation transition, magma ascent is induced by the density difference between ascending vesiculating magma and descending degassed magma. Above the transition, gas percolation will allow efficient outgassing without further expansion of bubbles. The viscosity of ascending magma will increase as it degasses, particularly after plagioclase formation begins at pressures <40 MPa. Therefore at superficial levels the viscosity contrast between ascending and degassing magma would decrease, and the flow may become more complex in nature. Petrological evidence for mixing in the shallow system is given by Sr isotope measurements of the crystal assemblage (Francalanci et al., 2005) and zonation bands commonly observed within plagioclase crystals (Landi et al., 2004). Plagioclase zonation suggests that bytownitic cores that form during ascent have a denser labradoritic rim grow around them in the shallow magma reservoir. When the degassed magma cycles back down the conduit a proportion mixes with ascending magma, producing a second bytownitic rim around the existing crystals. Several cycles such as this could produce the multiply-zoned plagioclase observed on Stromboli.

5. Conclusions

We have used the VolatileCalc model to determine H_2O and CO_2 solubilities of Stromboli magma at various pressures, constrained by both open-path FTIR measurements of quiescent degassing and melt inclusion data. This has allowed determination of the magma porosity and density as a function of pressure. Combining the derived density profile with estimates for the viscosity of degassed magma and a flow model we have determined the velocity of ascending magma as a function of pressure. Combining this information with the mass flow rate of magma determined from the SO_2 flux measured during 2006 on Stromboli allowed us to constrain the radius of the conduit, and how it varied with pressure. We conclude that the high vesicularity of magma would promote gas percolation, with a transition from closed-system degassing to gas percolation occurring at pressures between 100 MPa and 50 MPa. The observation of gas channels in explosion products from

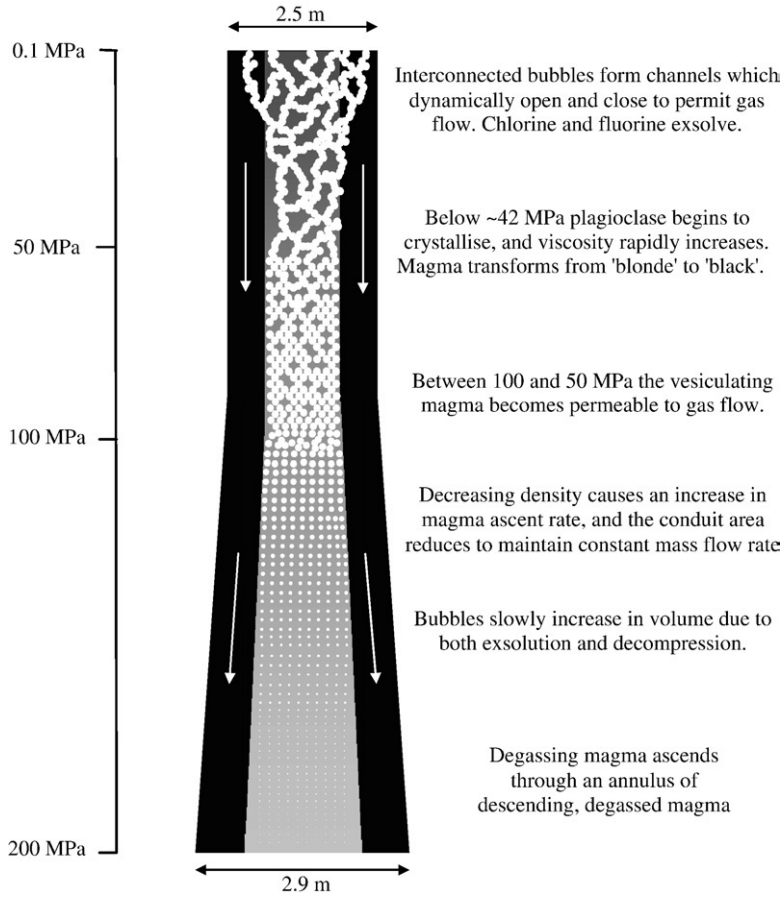

Fig. 7. Schematic model of degassing and magma circulation.

the shallow conduit is clear evidence for the presence of gas percolation.

A schematic picture capturing the essential features of the conceptual model proposed here is shown in Fig. 7. We believe this model may be generally applicable to persistent basaltic volcanoes systems that have sufficiently low viscosity to allow magma circulation, bubble growth and channel formation. The major factor which controls each system is the original dissolved volatile content, as this determines the depth of the transition to open-system degassing (more volatiles=>greater depth).

We have shown that a multidisciplinary approach to constraining the volcanic degassing system, combined with a fluid-dynamic model, can yield profound new quantitative insights into quiescent degassing processes. Subtle variations in these processes are likely to precede changes in volcanic activity, and therefore by improving our understanding of quiescent degassing we may greatly improve our ability to interpret measurements from volcano surveillance systems.

Acknowledgements

This work was supported by the National Institute of Geophysics and Volcanology, the Italian Civil Protection and DPC Project V6 Stromboli. We thank the SYRMEP group of Elettra Sincrotrone Trieste, Don Baker, Liping Bai and Livia Colò for help during tomographic experiments and J. Lowenstern and S. Vergniolle for their constructive reviews.

References

Allard, P., 1997. Endogenous magma degassing and storage at Mount Etna. Geophys. Res. Lett. 24, 2219–2222.

Allard, P., Carbonnelle, J., Metrich, N., Loyer, H., Zettwoog, P., 1994. Sulphur output and magma degassing budget of Stromboli volcano. Nature 368, 326–330.

Allard, P., Burton, M., Murè, F., 2005. Spectroscopic evidence for a lava fountain driven by previously accumulated magmatic gas. Nature 433, 407–410.

Armienti, P., Francalanci, L., Landi, P., 2007. Textural effects of steady state behaviour of the Stromboli feeding system. J. Volcanol. Geotherm. Res. 160, 86–98.

Barberi, F., Rosi, M., Sodi, A., 1993. Volcanic hazard assessment at Stromboli based on review of historical data. Acta Vulcanol. 3, 173–187.

Bertagnini, A., Métrich, N., Landi, P., Rosi, M., 2003. Stromboli volcano (Aeolian Archipelago, Italy): an open window on the deep-feeding system of a steady state basaltic volcano. J. Geophys. Res. 108, 2336–2350.

Blank, J.G., Brooker, R.A., 1994. Experimental studies of carbon dioxide in silicate melts: Solubility, speciation and stable carbon isotope behaviour. Rev. Mineral. 30, 157–186.

Blower, J.B., 2001. Factors controlling permeability–porosity relationship in magma. Bull. Volcanol. 63, 497–504.

Burton, M.R., Allard, P., Murè, F., La Spina, A., 2007. Magmatic gas composition reveals the source of Strombolian explosive activity. Science 317, 227–230.

Burton, M.R., Salerno, G., Murè, F., Caltabiano, T., in preparation. SO_2 flux measurements during 2005–06 on Stromboli determined using an automated UV scanner array.

Caricchi, L., Burlini, L., Ulmer, P., Gerya, T., Vassalli, M., Papale, P., in press. Non-Newtonian rheology of crystal-bearing magmas and implications for magma ascent dynamics. Earth Planet. Sci. Lett. doi:10.1016/j.epsl.2007.09.032.

Chouet, B., Hamisevicz, N., McGetchin, T.R., 1974. Photoballistics of volcanic jet activity at Stromboli, Italy. J. Geophys. Res. 79, 4961–4976.

Chouet, B., et al., 2003. Source mechanisms of explosions at Stromboli volcano, Italy, determined from moment tensor inversions of very-long-period data. J. Geophys. Res. 2019. doi:10.1029/2002JB001919.

Costa, A., 2006. Permeability–porosity relationship: a re-examination of the Kozeny–Carman equation based on a fractal pore-space geometry assumption. Geophys. Res. Lett. 33. doi:10.1029/2005GL025134.

Costa, A., Melnik, O., Sparks, R.S.J., 2007. Controls of conduit geometry and wallrock elasticity on lavadome eruptions. Earth Planet. Sci. Lett. 260, 137–151.

Eichelberger, J.C., Carrigan, C.R., Westrich, H.R., Price, R.H., 1986. Non-explosive silicic volcanism. Nature 323, 598–602. doi:10.1038/323598a0.

Francalanci, L., Tommasini, S., Conticelli, S., Davies, G.R., 1999. Sr isotope evidence for short magma residence time for the 20th century activity at Stromboli volcano, Italy. Earth Planet. Sci. Lett. 167, 61–69.

Francalanci, L., Davies, G.R., Lustenmhower, W., Tommasini, S., Mason, P., Conticelli, S., 2005. Intra-grain Sr isotope evidence for crystal re-cycling and multiple magma reservoirs in the recent activity of Stromboli volcano, southern Italy. J. Petrol. 46, 1997–2005.

Francis, P.W., Oppenheimer, C., Stevenson, D., 1993. Endogenous growth of persistently active volcanoes. Nature 366, 554–557.

Francis, P.W., Burton, M.R., Oppenheimer, C., 1998. Remote sensing measurements of volcanic gas composition by solar FTIR spectroscopy. Nature 396, 567–570.

Galle, B., Oppenheimer, C., Geyer, A., McGonigle, A.J.S., Edmonds, M., Horrocks, L., 2003. A miniaturised ultraviolet spectrometer for remote sensing of SO_2 fluxes: a new tool for volcano surveillance. J. Volcanol. Geotherm. Res. 119, 241–254.

Gaonac'h, H., Lovejoy, S., Shertzer, D., 2003. Percolating magmas and explosive volcanism. Geophys. Res. Lett. 30, 1559. doi:10.1029/2002GL016022.

Gardner, J.E., Burgisser, A., Hort, M., Rutherford, M., 2006. Experimental and model constraints on degassing of magma during ascent and eruption. Spec. Publ. — Geol. Soc. Am. 402, 99–113.

Giordano, D., Dingwell, D.B., 2003. Viscosity of hydrous Etna basalt: implications for Plinian-style basaltic eruptions. Bull. Volcanol. 65, 8–14.

Gonnermann, H.M., Manga, M., 2003. Explosive volcanism may not be an inevitable consequence of magma fragmentation. Nature 426, 432–435.

Harris, A.J.L., Stevenson, D.S., 1997. Magma budgets and steady-state activity of Vulcano and Stromboli. Geophys. Res. Lett. 24, 1043–1046.

Jaupart, C., 1998. Gas loss from magmas through conduit walls during eruption. In: Gilbert, J.S., Sparks, R.S.J. (Eds.), The Physics of Explosive Volcanic Eruptions. Geol. Soc., vol. 145. Sp. Publ., London, pp. 73–90.

Jaupart, C., Allegre, C.J., 1991. Gas content, eruption rate and instabilities of eruption regime in silicic volcanoes. Earth Planet. Sci. Lett. 102, 413–429.

Jaupart, C., Vergniolle, S., 1988. Laboratory models of Hawaiian and Strombolian eruptions. Nature 331, 58–60.

Jaupart, C., Vergniolle, S., 1989. The generation and collapse of a foam layer at the roof of a basaltic magma chamber. J. Fluid Mech. 203, 347–380.

Kazahaya, K., Shinohara, H., Saito, G., 1994. Excessive degassing of Izu–Oshima volcano-magma convection in a conduit. Bull. Volcanol. 56, 207–216.

Klug, C., Cashman, K.V., 1996. Permeability development in vesiculating magmas: implications for fragmentation. Bull. Volcanol. 58, 87–100.

Koyaguchi, T., Blake, S., 1989. The dynamics of mixing in a rising magma batch. Bull. Volcanol. 52, 127–137.

Landi, P., Métrich, N., Bertagnini, A., Rosi, M., 2004. Dynamics of magma mixing and degassing recorded in plagioclase at Stromboli (Aeolian Archipelago, Italy). Contrib. Mineral. Petrol. 147, 213–227.

Landi, et al., 2006. The December 2002 July 2003 effusive event at Stromboli volcano, Italy: insights into the shallow plumbing system by petrochemical studies. J. Volcanol. Geotherm. Res. 155, 263–284.

Lautze, N.C., Houghton, B.F., 2007. Linking variable explosion style and magma textures during 2002 at Stromboli volcano, Italy. Bull. Volcanol. doi:10.1007/s00445-006-0086-1.

Lautze, N.C., Houghton, B.F., 2005. Physical mingling of magma and complex eruption dynamics in the shallow conduit at Stromboli volcano, Italy. Geology 33, 425–428.

Llewellin, E.W., Mader, H.M., Wilson, S.D.R., 2002a. The rheology of a bubbly liquid. Proc. R. Soc. Lond., A 458, 987–1016.

Llewellin, E.W., Mader, H.M., Wilson, S.D.R., 2002b. The constitutive equation and flow dynamics of bubbly magmas. Geophys. Res. Lett. 29, 2170. doi:10.1029/2002GL015697.

Llewellin, E.W., Mader, H.M., Wilson, S.D.R., 2003. Correction to "The constitutive equation and flow dynamics of bubbly magmas". Geophys. Res. Lett. 30, 1340. doi:10.1029/2003GL017199.

Metrich, N., Allard, P., Spilliaert, N., Andronico, D., Burton, M., 2004. 2001 flank eruption of the alkali- and volatile-rich primitive basalt responsible for Mount Etna's evolution in the last three decades. Earth Planet. Sci. Lett. 228, 1–17.

Métrich, N., Bertagnini, A., Landi, P., Rosi, M., 2001. Crystallization driven by decompression and water loss at Stromboli volcano (Aeolian Islands, Italy). J. Petrol. 42, 1471–1490.

Mourtada-Bonnefoi, C.C., Mader, H.M., 2004. Experimental observations of the effect of crystals and pre-existing bubbles on the dynamics and fragmentation of vesiculating flows. J. Volcanol. Geotherm. Res. 129, 83–97.

Mueller, S., Melnik, O., Spieler, O., Scheu, B., Dingwell, D.B., 2005. Permeability and degassing of dome lavas undergoing rapid decompression: and experimental determination. Bull. Volcanol. 67, 526–538.

Newman, S., Lowenstern, J.B., 2002. VOLATILECALC: a silicate melt-H_2O–CO_2 solution model written in Visual Basic for Excel. Comp. Geosci. 28, 597–604.

Papale, P., 2005. Determination of total H_2O and CO_2 budgets in evolving magmas from melt inclusion data. J. Geophys. Res. 110. doi:10.1029/2004JB003033.

Parfitt, E.A., 2004. A discussion of the mechanisms of explosive basaltic eruptions. J. Volcanol. Geotherm. Res. 134, 77–107.

Parfitt, E.A., Wilson, L., 1995. Explosive volcanic eruptions—IX: the transition between Hawaiian-style lava fountaining and Strombolian explosive activity. Geophys. J. Int. 121, 226–232.

Pitzer, K.S., Sterner, S.M., 1994. Equations of state valid continuously from zero to extreme pressures for H_2O and CO_2. J. Chem. Phys. 101, 3111–3116.

Polacci, M., Corsaro, R.A., Andronico, D., 2006a. Coupled textural and compositional characterization of basaltic scoria: Insights into the transition from Strombolian to fire fountain activity at Mount Etna, Italy. Geology 34, 201–204.

Polacci, M., Baker, D.R., Mancini, L., Tromba, G., Zanini, F., 2006b. Three-dimensional investigation of volcanic textures by X-ray computed microtomography and implications for conduit processes. Geophys. Res. Lett. 33. doi:10.1029/2006GL026241.

Polacci, M., Baker, D.R., Bai, L., Mancini, L., in press. Large vesicles record pathways of degassing at basaltic volcanoes. Bull. Volcanol.

Rintoul, M.D., Torquato, S., 1997. Precise determination of the critical threshold and exponents in a three-dimensional continuum percolation model. J. Phys. A: Math. Gen. 30, 585–592.

Rust, A.C., Manga, M., 2002. Effects of bubble deformation on the viscosity of dilute suspensions. J. Non-Newton. Fluid Mech. 104, 53–63.

Rust, A.C., Cashman, K.V., Wallace, P.J., 2004. Magma degassing buffered by vapour flow through brecciated conduit margins. Geology 32, 349–352.

Saar, M.O., Manga, M., 1999. Permeability-porosity relationship in vesicular basalts. Geophys. Res. Lett. 26, 111–114.

Stevenson, D.S., Blake, S., 1998. Modelling the dynamics and thermodynamics of volcanic degassing. Bull. Volcanol. 60, 307–317.

Sur, A., Lebowitz, J., Kalos, J.M., Kirkpatrick, S., 1976. Monte Carlo studies of percolation phenomena for simple cubic lattices. J. Stat. Phys. 15, 345–355.

Vergniolle, S., Brandeis, G., 1996. Strombolian explosions. 1. A large bubble breaking at the surface of a lava column as a source of sound. J. Geophys. Res. 101, 20,433–20,448.

Vergniolle, S., Brandeis, J.G., Mareschal, J.-C., 1996. Strombolian explosions. 2. Eruption dynamics determined from acoustic measurements. J. Geophys. Res. 101, 20449–20466.

Wallace, P.J., 2005. Volatiles in subduction zone magmas: concentrations and fluxes based on melt inclusion and volcanic gas data. J. Volcanol. Geotherm. Res. 140, 217–240.

Woods, A.W., Koyaguchi, T., 1994. Transitions between explosive and effusive eruption of silicic magmas. Nature 370, 641–645.